F61: Nuclear magnetic resonance spectroscopy

Thimo Preis and Tobias Abele*
Ruprecht-Karls-Universität Heidelberg

26.03-30.03.2018

Abstract

The goal of this experiment is to test methods of nuclear magnetic resonance with two different NMR analyzers. In detail we want to determine the spin-spin and spin-lattice relaxation time for two samples with different concentrations of Gadolinium solved in water with the usage of the Bruker minispec p20 apparatus. Measurement of the former quantity is carried out via the spin echo as well as the Carr-Purcell method. With the same setup we furthermore measured the chemical shift of protons and used it to identify five different substances. The Bruker minispec mq7.5 is used for imaging measurements in one and two dimensions. One-dimensional processes such as the time dependent mixture of oil and sand are analyzed and two-dimensional imaging is used to map the inner volume of samples which contain oil or water.

I. Theory

1. Relaxation time

A macroscopic probe consists of many atoms, each of which with a nucleus carrying a spin and thus a magnetic dipole moment $\mu_I = \hbar\gamma_I\vec{I}$. The spins try to align either in a parallel or an antiparallel way with respect to an external magnetic field B_0. Restricting the discussion to protons we expect an effective magnetization in direction of $\vec{B}_0$ due to them having the tendency to occupy the energetically more favorable state, according to the Fermi-Dirac statistic. Disrupting the macroscopic magnetization from equilibrium will always lead to the same macroscopic magnetization after some time, because the system wants to minimize its total energy according to the principle of least action. This process is called relaxation and we distinguish between two different kinds of relaxation.[1] [7]

*Under the supervision of Minjung Kim

1.1 Spin-Spin relaxation T_2

The spin-spin relaxation is caused by the interaction between distinct spins amongst themselves. The transverse magnetization gets decreased via the dephasing of the coherent movement of the spin magnetic moments. The characteristic relaxation time of this process is called spin-spin relaxation time T_2. The Bloch equations describe the time evolution of the magnetization subject to relaxation. From them one can derive the time evolution of the transverse magnetization to be determined by the spin-spin relaxation time via [1]

$$M_\perp(t) = M_\perp^0 \, e^{-\frac{t}{T_2}} \tag{1}$$

1.2 Spin-Lattice relaxation time T_1

The spin-lattice relaxation time describes the interaction between the spins with the external magnetic field. The energy emitted by a system out of equilibrium dissipating to its equilibrium state, thus attaining an effective equilibrium magnetization, is absorbed by the lattice. The characteristic time scale of this relaxation process caused in this interaction is called spin-lattice relaxation time T_1. The time evolution of the magnetization component (anti-)parallel to the external magnetic field B_0 is again determined by the Bloch equations via the spin-lattice relaxation time to be [1] [7]

$$M_\parallel(t) = M_\parallel^0 \left(1 - 2\, e^{-\frac{t}{T_1}}\right) \tag{2}$$

2. Chemical shift

Chemical shift is, besides dipole-dipole interaction and internal coupling, one of the main internal interactions of magnetic dipole moments. It accounts for an additional magnetic field caused by the electrons surrounding the magnetic dipole moments of the nucleus. The factor of proportionality between the additional and the external magnetic field is molecule specific and is called magnetic shielding factor (measured in parts per million). The Hamiltonian of the observed system is given by

$$H = H_Z + H_C + H_J + H_D \tag{3}$$

where H_Z represents the Zeeman splitting caused by the external magnetic field B_0 and H_D accounts for the dipole-dipole interaction (is averaged out in fluids). The electrons weaken the magnetic field around the nucleus proportionally to the external magnetic field, following Lenzt's law, which in turn results in the chemical shift $H_C = \hbar\gamma\sigma\vec{I}\vec{B}_0$. The additional term $H_J = J_{12}\vec{I}_1\vec{I}_2$ is caused by the indirect coupling between two magnetic dipole moments in a molecule via the electrons, J_{12} describes the coupling factor. The Brownian motion is responsible for averaging out the splitting of the spectrum caused by the indirect coupling in different molecules.[3] [4]

3. Imaging with NMR

A static, spatially homogeneous magnetic field is not sufficient for image taking, because all spins would have the same Larmor frequency. One excitation pulse would therefore always excite the entire sample. We can spatially localize the amount of hydrogen atoms at one point by applying a gradient field, because the Larmor frequency is proportional to the magnetic field and which in turn is proportional to the spatial position. We can split the sample into slices in e.g. the xy-plane by applying a magnetic gradient in z-direction, because this results in the precession motion of every slice to have a different Larmor frequency:

$$\omega_{Larmor} = \gamma \left(B_0 + B^z(z) \right) \tag{4}$$

One can therefore guarantee spins of a specific slice to go in resonance with the frequency applied to the rotating magnetic field and then measure the relaxation time, this is called frequency coding. The stronger the applied magnetic gradient the thinner a given slice in the xy-plane becomes.
We can furthermore apply a phase encoding gradient to dephase spins along the vertical axis (y-axis). The gradient is only applied for a short amount of time such that, after the gradient has been shut down, we observe several phases between the spins along the y-axis, hence we now can decode the y-position via the phase with a spin echo measurement (compare 1.1), this is called phase coding. The resolution of this localization is limited by the measurement only being able to distinguish two phases with a difference less than 2π.
We can finally apply a third gradient field in x-direction during the echo, this results in the z-gradient field to increase along the x-direction such that the Larmor frequencies along the x-axis increase with an increase in magnetic field strength. The measured echo of the magnetic resonance signal now consists of a broad frequency spectrum, but now we can identify the spatial point via the specific Larmor frequency. One can now use either frequency or phase coding in order to acquire a 1D image of the sample via a 1D Fourier transformation of the measured NMR signal, where now every point in position space corresponds either to a specific frequency or a specific phase.
One can also use both methods in order to make a 2D image measurement. One first selects a slice by an appropriate combination of gradient field and high frequency pulse. Within the slice, 2D position information is derived by a combination of phase coding in x-direction and frequency coding in y-direction. One now proceeds to make N measurements, each consisting of a combination of frequency and phase coding, with different values of the phase coding gradients in x-direction. During every measurement the NMR signal is read out at different times t_m with $m \in \{1, M\}$. The 2×2D matrix of the image is then finally derived via a two dimensional Fourier transformation of the matrix consisting of $N \times M$ data points.[1] [9]

II. Experimental setup and measurement principles

1. Measurement of relaxation times and chemical shift

In the first part of the experiment the spin-lattice relaxation time T_1 and the spin-spin relaxation time T_2 are measured. The spin-spin relaxation time is measured by the spin echo (compare section 1.1) as well as by the Carr-Purcell method (compare section 1.2). The chemical shift of protons is measured in the following and used to identify five different substances. These measurements are carried out with a Bruker minispec p20, it consists of a Minispec p20 Electronic Unit used signal generation and of a Minispec p20 magnet with a static magnetic field B_0. The magnet is shielded by Styrofoam for minimal termperature variation when in use. One can now generate a magnetization $M_\perp$ perpendicular or $M_\parallel$ antiparallel to $\vec{B}$ by applying a high frequency pulse ω_{HF} via the electronic unit to the ground state magnetization $\vec{M}$. We can now rotate the macroscopic magnetization by an angle $\alpha = \gamma_I B_1 \Delta t$ by applying a sinusoidal voltage of given frequency ω_{HF} for a given time duration Δt to a coil oriented perpendicular to the static magnetic field B_0. This results in a solenoidal magnetic field $\vec{B}_1$ which is longitudinally polarized in a parallel way with respect to the orientation of the coil. The rotated macroscopic magnetization now precesses around the B_0 magnetic field. This in turn induces a voltage into the same coil, which then again represents our measurement signal, which is a mixed signal partially consisting of the so-called working frequency. It is the difference $\nu_{work} = \omega_{HF} - \omega_{Larmor}$ and it has to be calibrated to a value of around $1kHz$ by varying the Larmor frequency via varying the static magnetic field. The optimal Larmor frequency can be calculated with $\omega_{HF} = 19.8$MHz to be $\omega_{Larmor} = 19.799$MHz. The working frequency varied during the measurement by $\pm$50Hz due to variations in the magnetic field. With $\omega_{Larmor} = \gamma B_0$ we can therefore assume the magnetic field to vary by $\Delta B_0 \approx 5.2 \times 10^{-5} T$ whilst the temperature of the apparatus changed by $\Delta T \approx 0.01$ °C. Thus, the systematic error in the calibrated working frequency due to temperature variations can be estimated to be around $\Delta\nu_{work,sys} = 5\%\nu_{work}$.
One can vary the time duration of the applied voltage in order to rotate the magnetization by an angle $\alpha = 90\,^\circ, 180\,^\circ$ into its perpendicular or antiparallel component with respect to the orientation of $\vec{B}_0$.[1]

1.1 Spin echo

In order to measure the spin-spin relaxation time T_2 according to equation 1 one starts with a $90\,^\circ$ pulse in order to create a transverse magnetization in y-direction, such that it will precess around the static magnetic field B_0 with a given Larmor frequency $\omega_{Larmor} = \gamma B_0$.

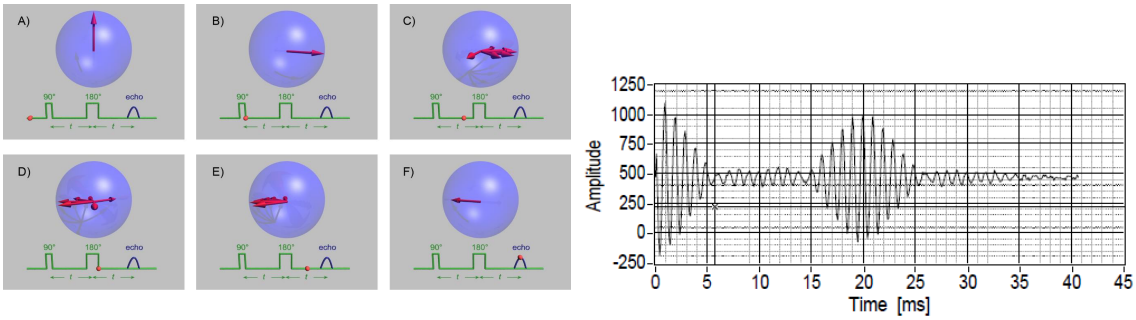

Figure 1: *From left to right: Spin echo method [6], output signal [1]*

Protons at different positions in the probe will now precess with different Larmor frequencies due to the non-linearity of the field, thus phase difference between the protons will develop. One can now revert the phases of the spins with a 180° pulse in order to guarantee all protons of given phases to coherently align after a given time interval of two times the so-called spin-echo time τ. The induced signal then again represents the relaxation time for the transverse magnetization, which is dominantly caused by spin-spin interactions, thus T_2. [1] [7]

1.2 Carr-Purcell sequence

One only achieves approximate alignment of the magnetic dipole moments after 2τ for long spin echo times due to molecular diffusion happening before the 180 ° pulse can be applied. The Carr-Purcell sequence minimizes the effects of molecular diffusion and field inhomogeneities by starting the sequence with a 90 ° pulse followed up by a 180 ° pulse to ensure phase coherence of the system after $t = 2\tau$. One now applies further 180 ° pulses for every odd multiple of τ in order to guarantee phase coherence for every even multiple of τ. A measurement of the spin-spin relaxation time by the Carr-Purcell

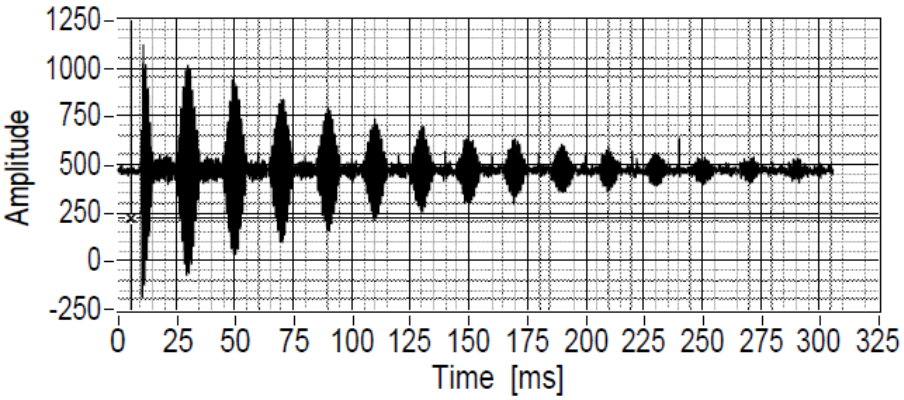

Figure 2: *Carr-Purcell sequence [1]*

method hence yields a value which is closer to the true value of the system as compared

to the measurement with the spin echo method.[1]

1.3 Measurement of spin-lattice relaxation T_1

One produces a magnetization antiparallel to the static magnetic field by starting the measurement with the generation of a 180 ° pulse. By following this up with a 90 ° pulse one measures a signal which represents the current longitudinal magnetization, which is due to spin-lattice interactions and can therefore be used to measure T_1.[1]

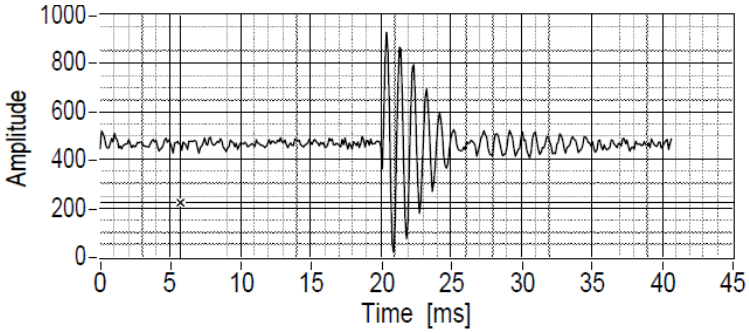

Figure 3: *Pulse sequence 180 °-90 °with τ = 20ms [1]*

2. Imaging with NMR

The imaging measurements are made with the Bruker NMR analyzer mq7.5, where the gradient fields where applied via a system of Helmholtz coils. Nuclear Magnetic Resonance techniques are used for imaging measurements in one and two dimensions. The flow of oil in sand is measured as a time dependent process in one dimension. Two dimensional measurements are carried out to map the inner volume of substances which contain oil or water. The measurement principle of this apparatus is described within section 3.[1]

III. Data analysis

1. Measurement of relaxation times

Both the spin-spin and the spin-lattice relaxation time have been measured with the use of two different concentrations of Gadolinium solved in water, one solution with 500 water molecules per Gadolinium atom (Gd500) and the other solution containing 600 water molecules per Gadolinium atom (Gd600). The measured values were acquired by a fit of their respective fit functions(compare equation 1 for T_2 and equation 2 for T_1) applied to the measured data as seen in figure 4
Pulse I has to be maximized in order to represent a 90 ° pulse, it was set to $\approx$ 2.1, and Pulse II has to be minimized in order to be a 180 °, it was set to $\approx$ 2.2. We aquired a data point at 900ms echo time for the T_1 Gd500 measurement which we decided to

	Gd500	Gd600
T_2	$(99.8 \pm 0.5_{stat})$ ms	$(129 \pm 1_{stat})$ ms
T_2(CP)	$(124.0 \pm 0.4_{stat})$ ms	$(150.6 \pm 0.6_{stat})$ ms
T_1	$(118.8 \pm 2.2_{stat})$ ms	$(251.9 \pm 4.7_{stat})$ ms

Table 1: *Measured Values*

exclude from the fitted dataset as it was way higher than one would theoretically expect. We found the reason for this to be the sensitivity of the measurement configuration to the background noise, because we changed the integrated over peak window before the aquirement of said data point. One theoretically expects T_2(CP) to be larger than T_1 for both solutions, because the spin-spin interaction dominates T_2: Dipoles want to align in the energetically most favourable way, antiparallel. This alignment proceeds faster in comparison to the spin-lattice interaction important for the T_1 measurement. T_1 describes the average time needed for the mean magnetization to go over from antiparallel to parallel alignment with respect to the external magnetic field, this is microscopically described by single spins orienting themselves from $-1/2$ to $+1/2$.[1] We observe our expectation of T_2 (CP) being larger and more precise than T_2, as explained in 1.2, to be true.

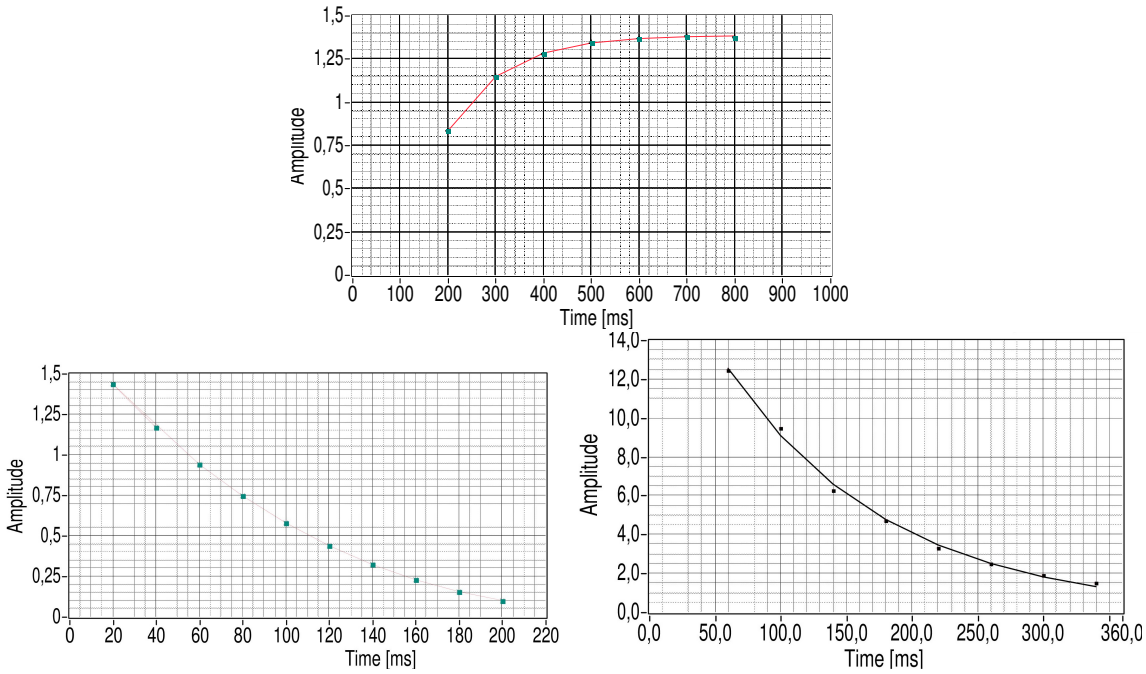

Figure 4: *In the top row: spin-lattice relaxation time T_1 in Gd500 with spin-echo method*
From left to right in the bottom row: spin-spin relaxation time T_2 in Gd500 with spin-echo method and spin-spin relaxation time T_2 in Gd500 with the Carr-Purcell (CP) method

We furthermore observe the relaxation times of Gd500 to be shorter than for Gd600. Gadolinium is strongly paramagnetic and is magnetized at room temperature (Curie point at $\approx$ 19 °C). The form of paramagnetism exhibited by Gadolinium compounds derives from electrons, not protons, and is known as Curie Paramagnetism. Because of electrons having $s = 1/2$, but a much smaller size than the proton, their gyromagnetic ratio is $\approx$ 657 times larger. If the electrons remain unpaired in shells or bonding orbitals, the unbalanced spin produce a strong magnetic moment capable of inducing magnetic relaxation in nearby nuclei. The seven unpaired electrons in the $4f \rightarrow s_e = 7/2$ subshell therefore account for the elements strong paramagnetism. [2] The presence of such large fluctuating paramagnetic moments in a solution thus has strong effects on the nuclear spin relaxation of the solvent water nuclei. Therefore, the more Gadolinium atoms available the more dipole-dipole interactions between the water molecules and the Gadolinium atoms are possible and the shorter is the relaxation time. Instead we measured exactly the opposite to be true as can be seen in table 1. We therefore repeated our measurement for T_2(CP) and for T_1 with the Gd600 probe and a more narrow peak window to further exclude background noise. T_2(Cp) did not change much, but the new value for T_1 increased such that it met our theoretical expectations. We hence replaced the first measured value of $T_1 = (135.8 \pm 1.2_{stat})$ ms with the second measured value in table 1. Thus, again the use of the same configuration with a slightly more narrow peak window leads to a huge difference in measured values. Furthermore, we excluded the data produced for a spin echo time below $t = 200ms$, because the fit could not account for these as they were reflected across the time axis such that the measured values actually started with a decreasing trend until the zero crossing of the amplitude was met at around $t = 200ms$. Thus, the systematic deviation of T_1 from our theoretical expectation is due to an incomplete data set and due to the whole setup being very sensitive to the integrated over peak window, which hence should be checked quite thoroughly in order to guarantee reproducibility of results in this section.

2. Chemical shift

In order to identify the different simples A-E with the given chemical substances (Toluene, P-Xylene, Acetic acid, Fluoroacetone, Fluoroacetonitril) we applied a 90 ° pulse on the respective samples and acquired via Fourier transformation a frequency spectrum as output signal in which the different Larmor frequencies where observable.
The sample was put into a rotating motion via compressed air in order to average out non-linearities within the external magnetic field - the respective peaks got clearly more narrow and more distinct. Rotating the sample near the relaxation time though messes up the system such that we constantly calibrated the applied working frequency after every measurement to be at the order of $\nu_{work} = (506 \pm 20)$Hz. This was also necessary, because the experimental setup is not isolated very well such that drifts in the magnetic field due to temperature variation are, despite the short measurement time, not preventable. We furthermore measured samples A+-E+ which additionaly contained

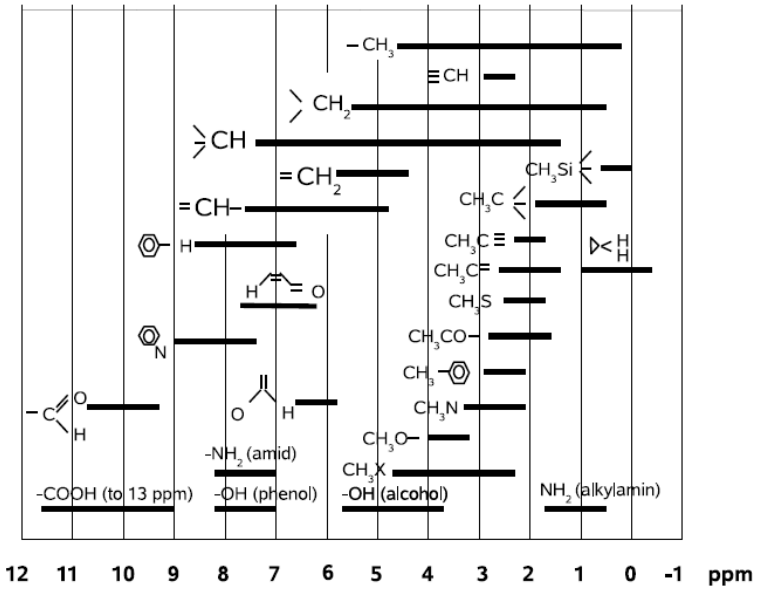

Figure 5: *Chemical shift of compounds relative to TMS [1].*

the substance Tetramethylsilane (TMS). The hydrogen resonance line of TMS is located near the edge of the shown spectrum due to its high chemical shift, we can thus use this line as a reference in order to distinguish between different samples. With the difference between the peaks of the respective samples and the reference peak we can identify every sample via figure 5. For sample A+ and D there were no corresponding samples with/without TMS available such that we identified the TMS reference peak via the samples B+, C+, E+. We found the ppm position of said peak by averaging said samples to be at $TMS = (31.30 \pm 0.12_{stat})$ ppm. This value can in the following be used as a reference value for the sample D, where no D+ sample was available, and for identifying the reference value for A+, where no sample A was available.
In the following analysis one has to be aware of CO not producing any resonance peak due to its nucleus having spin zero. We furthermore excluded CN from our evaluation as its resonance peak lies outside our reference window of -1 to 12 ppm as defined by figure 5.

Peak	frequency [Hz]	ppm	difference to TMS	Substance
1	484.0	24.4	6.2	FCH_2
2	530.0	26.8	3.8	FCH_2
3	560.0	28.3	2.3	CH_3
4	606.0	30.6	Reference	

Table 2: *Sample A+*

Sample A is from table 2 identified as Fluoroacetone. Fluorine atoms have an odd number

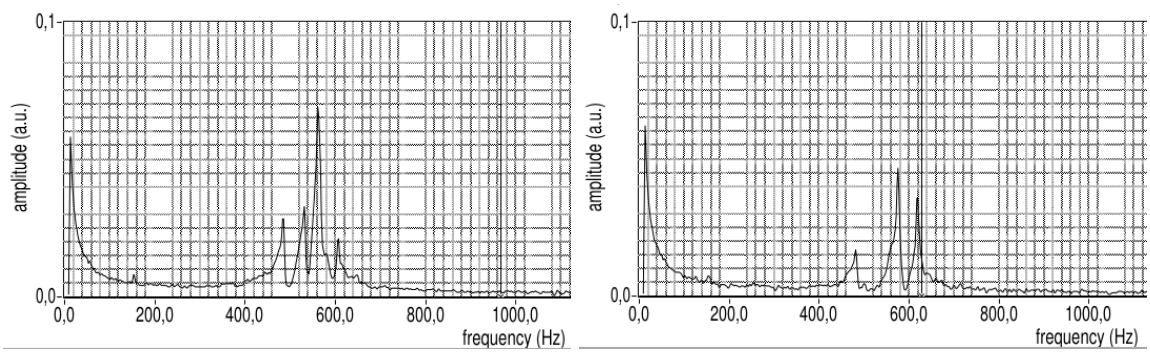

Figure 6: *Frequency spectrum of the A+ (left) and of the B+ (right) sample*

of protons and an even number of neutrons in their nucleus such that they posses a nuclear spin of $s = 1/2$, this spin can couple in a parallel or antiparallel way with respect to the orientation of the protont's spin of the CH_2 compound, such that we can observe two peaks belonging to FCH_2.[8]

Peak	frequency [Hz]	ppm	difference to TMS	Substance
1	480.0	24.2	6.9	Benzene
2	574.0	29.0	2.1	CH_3
3	616.0	31.1	Reference	

Table 3: *Sample B+*

Sample B could either correspond to Toluene or to P-Xylene. By comparison with sample E+ we find the intensity of peak 2 in table 3 to be much larger than its corresponding value of sample E in table 6, such that we identify sample B as P-Xylene.

Peak	frequency [Hz]	ppm	difference to TMS	Substance
1	386.0	19.5	11.6	COOH
2	573.9	29.0	2.1	CH_3
3	616.0	31.1	Reference	

Table 4: *Sample C+*

From table 4 we identify sample C to be Acetic acid.

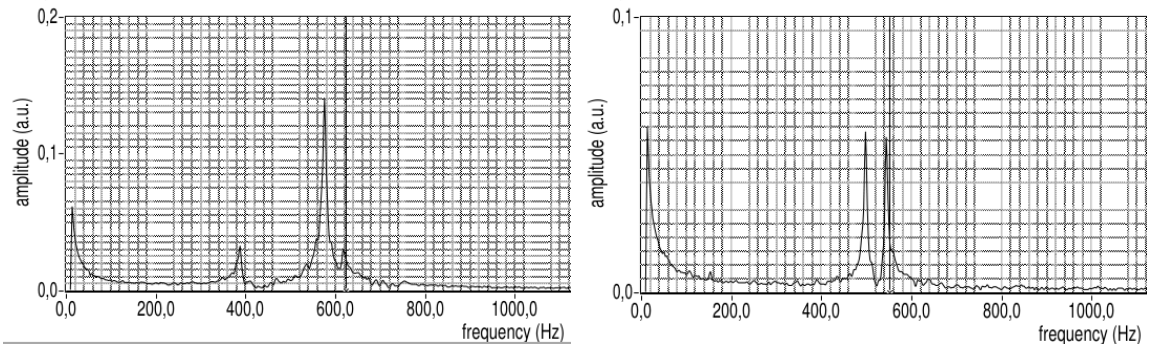

Figure 7: *Frequency spectrum of the C+(left) and of the D (right) sample*

Peak	frequency [Hz]	ppm	difference to TMS	Substance
1	496.0	25.1	6.2	FCH_2
2	542.1	27.4	3.9	FCH_2
3	31.30 ± 0.12	31.1	Reference from E+, C+, B+	

Table 5: *Sample D*

As for sample A (compare table 2) Fluorene couples either in a parallel or antiparallel way with respect to the protont's spin of the CH_2 compound such that we observe two peaks of different frequency corresponding to the same molecule. We therefore identify sample D from table 5 to be Fluoroacetonitril.

Peak	frequency [Hz]	ppm	difference to TMS	Substance
1	482.0	24.3	7.1	Benzene
2	580.0	29.3	2.1	CH_3
3	622.0	31.4	Reference	

Table 6: *Sample E+*

As discussed with sample B+ we identify sample E through comparison with table 3 to be Toluene.

3. Imaging with NMR

3.1 One dimensional imaging

The first two samples consisted of two glass tubes filled with 15mm and 50mm of oil respectively. The former sample produced a step function as output signal and the latter sample also produced a step function but with a broader width. We furthermore observe both samples to show different amplitudes in output signal due to non-linearities of the

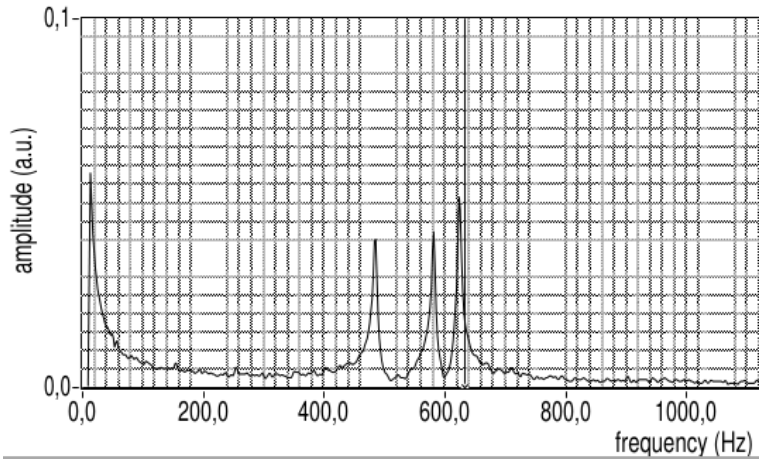

Figure 8: *Frequency spectrum of the E+ sample*

magnetic field and, furthermore, we observe both signals to be distorted by noise due to making a Fourier transformation of a finite dataset. The resulting images can be seen in figure 9.

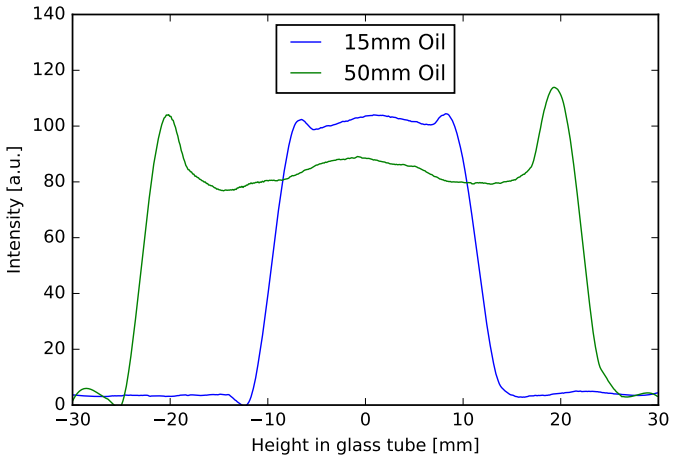

Figure 9: *1D imaging of 15 mm and 50 mm oil samples*

The next sample contained a cylindrical piece of teflon in the form of seven concentric, similar, equidistant and parallel slices surrounded by oil. The aquired spectrographic image in figure 10 shows diminished amplitudes in the center of the signal, because the seven slices are connected to a piece of plastic which holds said slices in place and which gives no signal. We can furthermore deduce from figure figure 10, that the thickness of the Teflon layers ($\approx$ 1.5mm) is larger than the resolution of the Brucker NMR analyzer mq7.5 used in this setup, otherwise we would simply observe a step function for the whole sample due to the resolution not being high enough to show the oil layers in between

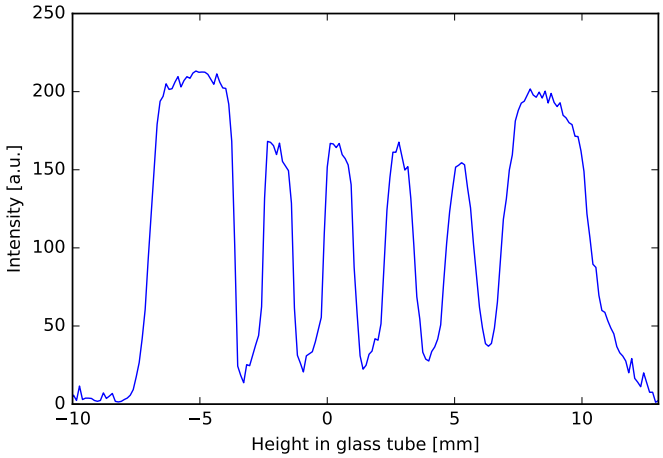

Figure 10: *1D imaging of an oil sample mixed with Teflon layers*

the teflon slices. The resolution of the Bruker NMR analyzer mq7.5 was given by the manual to be $<$ 1mm. It is limited by the least possible step size of the magnetic field in the measurement being quite large, such that one cannot distinguish in small ranges of B, and by only performing a Fourier transformation of a finite set of datapoints, which in turn results only in an approximate representation of the input signal due to the Fourier transformation of the step function (hyperbolic sine) only having a finite number of main oscillations in the given dataset.
The fourth sample contained 15 mm of sand and approximately 4mm of oil on top. In the following we will answer the question whether this process of oil mixing with sand can be understood as a diffusion process. Figure 11 shows the measured data aquired in steps of 2 minutes in between every plotted line. The signal at first is simply a step-function with some background noise, which represents the input signal from the separated oil layer. The zero point on the x-axis therefore gives us the border between the oil and sand layer. The signal in the $x < 0$ area gradually increases over time as the oil sinks more and more into the sand layer. The signal at the end of the mixing process should be a flat, noisy step function as it should represent one signal for the whole oil-sand mixture. We instead observe it not being completely flat, but having some small bumps in between. This is due to tightly bound sand granules in between the mixture which do not let the oil sink through to the bottom side of the glass tube, these areas therefore give no signal. The mixing of oil and sand observed here would describe a diffusion process, if it would fall of like a convex function, compare [5]. We on the contrary measured this process to fall off in parts like a convex and in parts like a concave function, as seen in figure 11, such that we cannot deduce solely from this measurement, whether this process actually describes a diffusion process.

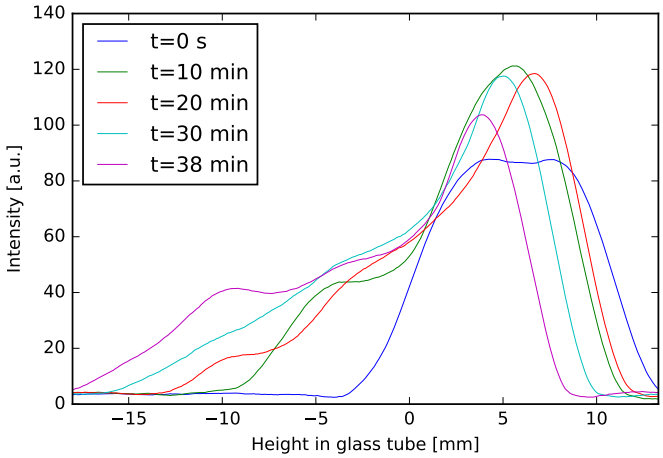

Figure 11: *Time dependent evolution of oil sinking into sand*

3.2 Two-dimensional imaging

The first sample consisted of 15mm oil within a glass tube. For horizontal slicing we expected a circle, as the sample gives a signal at every point until the boundaries of the glass tube are met. The result can be seen in figure 12. The distortion of the circular image to the front is due to non-linearities of the magnetic field intrinsic to this machine, we therefore concluded not to use back to front slicing in the following with this setup.

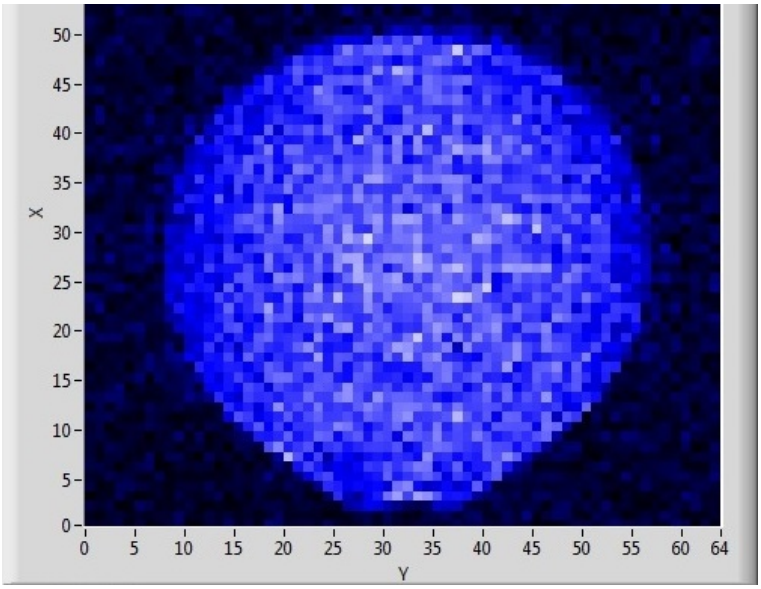

Figure 12: *15mm oil sample sliced back to front horizontally*

We expect a square to show for left to right slicing, again due to the sample consistently

giving a signal until the boundaries of the glass tube are met. The result of the left to right slicing can be seen in figure 13. The curve at the top of the slice is due to surface tension

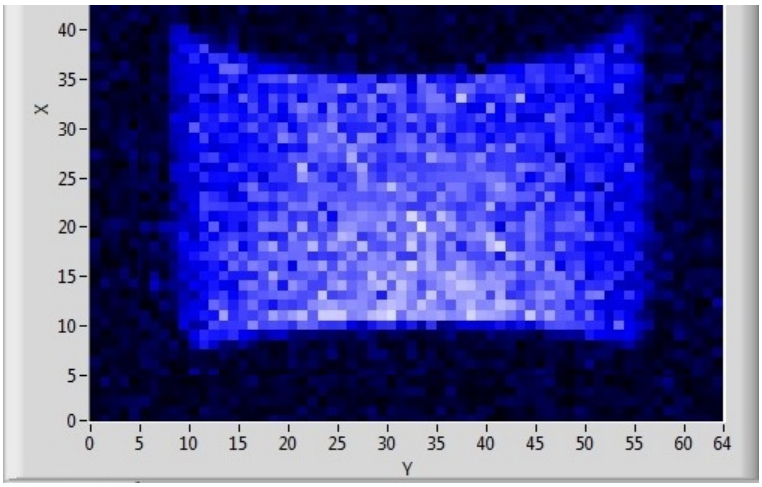

Figure 13: *15mm oil sample sliced vertically from left to right*

between the oil and the glass tube. The flat edge at the bottom is due to the bottom side of the glass tube. Throughout the measurement we constantly checked the temperature in the Bruker NMR analyzer mq7.5, it stayed nearly constant and only changed by 0.001 °C.

We proceeded with taking twodimensional images of organic objects.
Figure 14 shows a peanut with shell. We can only observe one nut (the dark, elliptical object inside the upper cell), because the peanut was not completely centered in the glass tube such that the left to right slice only slices through one of the cells (the upper one with the nut shown) and only captures the beginning of the lower cell as the slice went right through the middle between the two cells.
Figure 15 shows the C-shaped form of a piece of celery. This is the second image taken from the same sample as the first one only showed unidentifiable structure, because here no perfect gradient could be calibrated due to the sample not being placed perfectly inside the measurement boundaries of the Bruker NMR analyzer mq7.5.
Figure 16 in contrast shows an apple core sliced horizontally. The star shaped core contains apple seeds which do not give any signal, hence the black areas. The signal of the area around the core comes from the pulp around it, it was partially cut off such that the shown shape is not perfectly circular.

IV. Discussion - Thimo Preis

The setup in the first two parts of the experiment was not isolated very well thermally such that the B_0 magnetic field was very sensitive to work with. The skew available for varying B_0 is furthermore very unprecise and does not increase or decrease B_0 consistently with a consistent rotating motion. It was therefore very difficult to calibrate the working

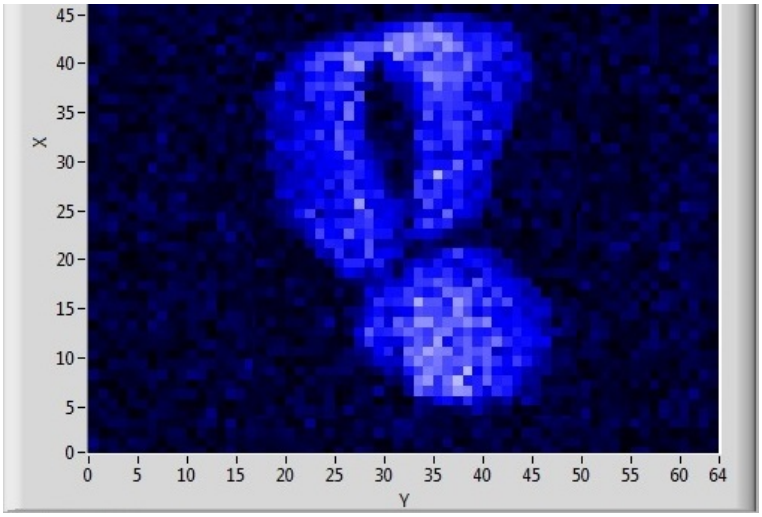

Figure 14: *Peanut inside shell sliced vertically from left to right*

frequency, which again is only necessary due to the ineffective thermal shielding with styrofoam, consistently after every measurement due to the unprecise adjustability of B_0. One should therefore improve the thermal shielding of the Minispec p20 magnet in order to render the ongoing calibration of the working frequency after every measurement unnecessary in the boundaries of the setups precision. One should furthermore increase the number of possible data points for the used fit of T_1 and T_2 in order to increase the precision of the measured values. This can easily be achieved by expanding the available LabView program to guarantee more than ten data points to be accounted for in the fit. One could furthermore refine the step size of the switches of the Minispec p20 electronic unit in order to account for more data points in the steeply falling/rising range of the exponential decay/rise. In total it would improve the precision of the measured results, if one would simply increase the number of taken data points during the measurement and also increase the number of measurements and thus improve on the fits in order to average out the huge systematic errors due to the sensitivity of the apparatus on the chosen peak window and on the thermal shielding. One should furthermore be provided with theoretical values of the relaxation times in order to guarantee a successfull discussion of the measured values and a prompt error evaluation during the experiment for measured values way off the theoretical values. These error sources had a higher impact on the first part of the measurement than on the second part concerned with the chemical shift. The systematic errors averaged out due to the structure of the measurement relying only on differences between the peaks.

The third part of the experiment went very smooth as the Bruker NMR analyzer mq7.5 was thermally shielded very well (compare 3.2) and had a high image resolution, only the intrinsic magnetic field non-linearities distorted our images a bit. By trying out the different slicing methods we could nevertheless achieve images of high resolution from

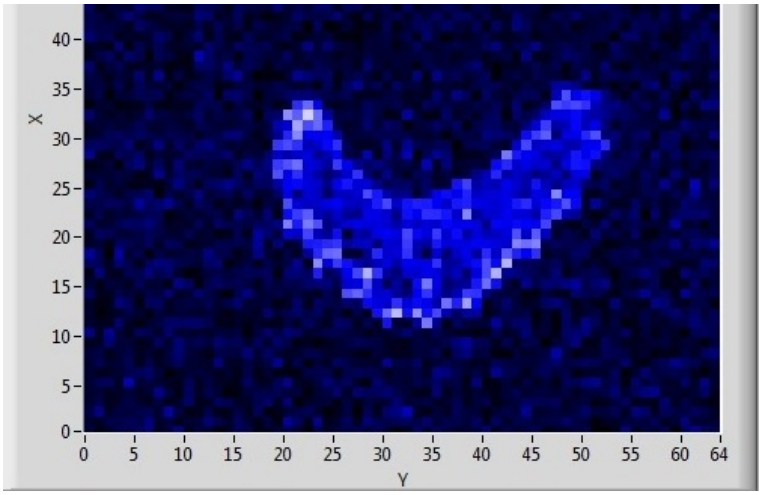

Figure 15: *Sample of celery sliced horizontally*

which we could draw important physical conclusions.
The instruction manual [1] gives a clear introduction to the NMR concepts. The third part concerned with "Imaging with NMR" is to in depth for this experiment and misses to convey the quintessential points of this method. One should therefore cut down the explanation of the actual Fourier transformation of the NMR signal and in contrast should go more in depth in explaining the actual two dimensional data aquisition and on how the Helmholtz coils were set up in order to guaruantee linear gradient fields.
Altogether this experiment is very instructive in conveying the import NMR methods used throughout the medical and food sector in an engaging way. Only the first part of the experiment could be improved in order to increase the precision of the measured results as discussed above.

V. Discussion - Tobias Abele

In the first two parts we used a setup being isolated by Styrofoam. This of course isolates, but not as good as one would expect an isolation for an advanced practical course.
One had to use several plates of Styrofoam to isolate the setup, which provides much more possibilities for exchange of thermal energy than a complete box of Styrofoam. The room temperature influenced the magnetic field we had to adjust, which made the already quite difficult adjustment of the field even less accurate or stable. Turning the adjustment wheel always in one direction changed the magnetic field in long-time range either up or down, but for small adjustments the field sometimes went up and then down, which made corrections for the working frequency after each measurement due to thermal exchange complicated. Either more adjustments or simply a better thermal isolation of the whole setup for the first two parts would improve our measurements significantly. Additionally, it would have helped, if one would have known what changing the adjustment wheel really changed and why the values sometimes went up or down when readjusting the

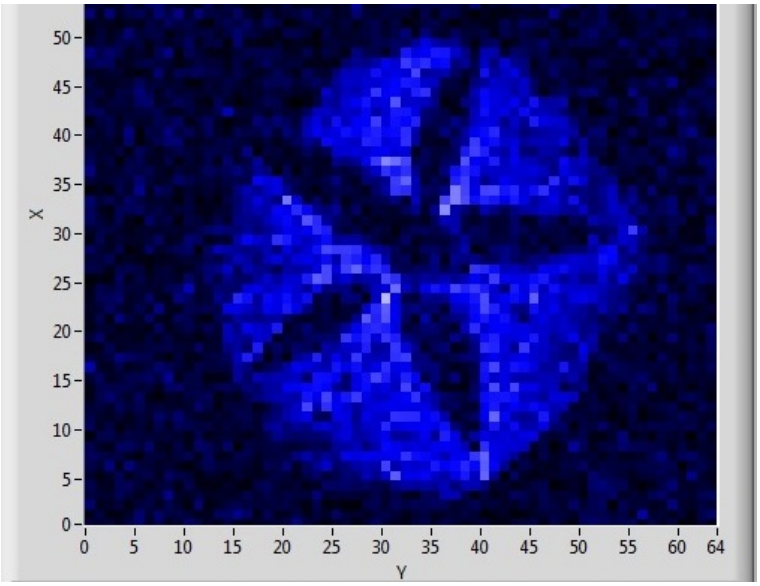

Figure 16: *Sample of an apple core sliced horizontally*

field. An improvement for the used program LabView would be a change in the step size of switches of the used Minispec 20 and a measurement of more data points to improve the fits and lower statistical errors.
Some reference values would improve the measurement, too.

When measuring the chemical shifts, some changes of peaks appeared due to readjustments of the magnetic field because of exchange of thermal energy. But all in all, the measurements of this part were fine. Only the noise of the pressure air one could improve with a motorised setup spinning the glass tubes of the different probes electrically and not mechanically due to air.

For the third part, the imaging part of this experiment, we used another setup, the Bruker NMR analyzer mq7.5, which was isolated thermally very well. Some magnetic field non-linearities skewed some of our pictures. Another problem was the very small tube for own probes, which provided us some extra work when preparing the measurement with the apple core. But solving this problem would result in a new and bigger NMR analyser, which probably is too expensive. An improvement as well could be another probe, which refers a little more to the medical use of the NMR technique such as probes of organisms.

Another aspect is the manual, which was fine until part three. Here it was too detail-obsessed and only very confusingly explained the theoretical principle of this part. A greater depth in the part of the two-dimensional data acquisition instead would ease the experiment for other groups in the future.

To summarise, the experiment was very insightful and interesting to get to know the widely used NMR technique better and deepen knowledge connected with the theory behind it. One could just improve the first part by improving the setup and the second part by cutting and improving the manual as discussed above.

References

[1] F61 - Nuclear Magnetic Resonance in the Advanced Students Laboratory. Url: https://www.physi.uni-heidelberg.de/Einrichtungen/FP/anleitungen/F61.pdf

[2] Gadolinium Wikipedia article, Last Access: 02/04/2018 20:24, Url: https://en.wikipedia.org/wiki/Gadolinium

[3] The Basics of NMR by Joseph P. Hornak URL: http://www..cis.rit.edu/htbooks/nmr

[4] Indirect dipole-dipole coupling, Last Access: 02/04/2018 20:24, Url: https://en.wikipedia.org/wiki/J-coupling

[5] Diffusions-Poren-Bildgebung mittels kernmagnetischer Resonanz" Dissertation of Tristan Anselm Kuder, University Heidelberg(2014)

[6] Spin echo method, Last Access: 02/04/2018 20:24, Url: https://en.wikipedia.org/wiki/Spin_echo

[7] Wie funktioniert MRI? By Weishaupt, Dominik in Springer 2014, ISBN: 978-364-24161-6-3

[8] Fluorine atom information, Last Access: 02/04/2018 20:24,Url: https://en.wikipedia.org/wiki/Fluorine

[9] Principles of nuclear magnetic resonance in one and two dimensions by Ernst, Richard R and Bodenhausen, Geoffrey and Wokaun, Alexander and others. Volume 14, 1987, Clarendon Press Oxford.